Relaxation Phenomena of the Concentration Polarization in High Temperature Air Cathodes

Tadao KENJO* and Yukiyasu YAMAKOSHI
Department of Applied Chemistry, Muroran Institute of Technology,
Mizumoto-cho, Muroran 050
(Received November 3, 1991)

The transient depolarization curves of Pt/ZrO_2 high temperature air cathodes have been measured and compared with theoretical curves calculated by assuming a diffusion mechanism of atomic oxygen. The decay equation used involves the limiting current density, time constant for the decay rate and effective reaction area, as parameters to be determined. These parameter values were obtained by curve fitting. The polarization loss was found to decrease with increasing O_2 pressure at the rate expected from the diffusion mechanism. The performance of the electrodes was enhanced as the sintering temperature rose. This trend was reflected on an increase in the parameter of effective reaction area. The performance was improved by loading an excess current. This effect was explained as being due to an increase in the diffusivity of O_a.

Recently, there are increasing interests in the high temperature solid oxide fuel cells (SOFC) which are expected to provide high efficiency. However, calculations performed recently indicate a lower efficiency than expected at the beginning of the SOFC study.[1] For further efficiency improvements, knowledge on the loss mechanism and the proportion of each loss involved in the SOFC is required.

The ohmic loss is a major voltage loss, which can be separated from the total loss by the current interruption method.[2] It is based on the difference in the decay rate of the electrode potential for rectangular current pulses: When the DC current is interrupted, the ohmic loss drops instantaneously, whereas the activation polarization decays gradually with a rate depending on the time constant associated with the electrochemical process. Separation of the ohmic loss and activation polarization can thus be made readily by a current interrupter installed with an oscilloscope which can measure a time gap $<10^{-7}$ sec.

The decay curves following the instantaneous ohmic drop are ascribed to the charge-transfer polarization and/or concentration polarization. Since the time constants of these two polarization processes are close to each other, separation of the two is not so easy as that of the ohmic drop from the total loss. In most of the studies on the high temperature cathodes that have so far been made, the decay curves are interpreted as a discharge of the parallel R–C circuit.[3,4] The physical meanings of R and C involved in the circuit are the charge-transfer polarization and double layer capacity, respectively. This circuit cannot therefore be applied to the decay process where the concentration polarization predominates. In fact, appreciable deviations have been observed between the experimental decay curves and theoretical ones calculated from the R–C circuit,[3] particularly when the decay curves are taken over a relatively long time range. To correct these deviations, we have carried out a numerical calculation of a decay equation involving a term for the concentration polarization which is controlled by the dissociation of molecular oxygen.[5] The present study is an attempt to study the case for the diffusion controlling.

When the diffusional loss is a major polarization component, the decay curve should be described in terms of a transient increase of oxygen concentration, from the concentration in the steady state to that in the equilibrium state. The time variation of the oxygen concentration at the three phase boundary is expressed by Fick's second law. In this study, a decay equation will be given as an approximate solution of Fick's differential equation. Parameters involved in the equation are determined by curve fitting. The analytical method is applied to Pt/ZrO_2 electrodes prepared in various conditions to see the reason why the electrode performance varies with the preparative conditions.

Experimental

Electrodes and Electrolytes. The electrolytes used were yttria-stabilized zirconia (YSZ) disks, which were prepared by sintering green pellets of YSZ fine powder (Toso Co., Ltd., TZ-8Y, 8 mol% Y_2O_3) at 1500 °C for 3 h in air. The disks obtained were approximately 3 cm dia. and 1.5 mm thick.

The electrodes used were platinum paste electrodes. Both the cathode and anode were prepared by painting a fluxless platinum paste (Tokuriki Chemical Research Company, No. 8103) over a 2 cm^2 area on the electrolyte disks and then heating them usually at 1000 °C for 1 h in air. A reference electrode of the same platinum paste was painted onto a peripheral area of the disk.

Measurements of Decay Curves. Decay curves were measured at 900 °C usually in air, but Ar–O_2 mixed gas was used for measuring the dependence of O_2 pressure. The current interruption circuit for the measurement of the decay curve is shown schematically in Fig. 1. The rectangular pulses were supplied from a pulse generator with a frequency of 1-10 Hz. This pulsed current was applied to the test cell and the resulting potential was measured against the reference electrode on the oscilloscope screen. The initial potential value after the instantaneous drop due to the ohmic drop was regarded as the steady-state polarization loss. The decay

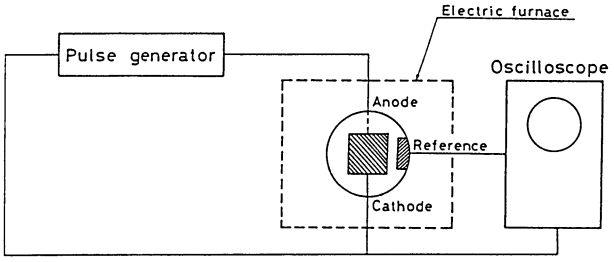

Fig. 1. Circuit diagram for the measurement of decay curves.

curve was taken from the gradually decreasing tail by reading the scale of the screen, and used for the following mathematical analysis.

Analysis of Decay Curves

The porous platinum electrodes used in the study are assemblies of small platinum particles sintered on the electrolyte face. The electrochemical O_2 reduction starts with the dissociative adsorption of O_2 molecules on the platinum surface

$$O_{2,g} \rightarrow 2O_a \tag{1}$$

where the subscripts g and a denote gas phase and adsorbed species, respectively. The atomic oxygen then diffuses to the three phase boundary (electrode–electrolyte interface). The charge transfer reaction takes place there as follows,

$$O_a + 2e^- \rightarrow O^{2-}. \tag{2}$$

The current density produced by the reaction can be expressed by the Butler–Volmer equation, in accordance with a similar reaction for liquid electrolyte,[6]

$$i = i_0\left\{\left(\frac{\theta}{\theta_0}\right)\exp\left(\frac{2\beta F}{RT}\eta\right) - \left(\frac{1-\theta}{1-\theta_0}\right)\exp\left(-\frac{2(1-\beta)F}{RT}\eta\right)\right\}, \tag{3}$$

where η is the total polarization loss, θ and θ_0 are the surface coverages of O_a in load and equilibrium conditions, respectively, and the other symbols have the usual meanings (see Nomenclature). Equation (3) can be changed to the form

$$i = i_0\left[\exp\left\{\frac{2\beta F}{RT}\eta + \ln\left(\frac{\theta}{\theta_0}\right)\right\} - \exp\left\{-\frac{2(1-\beta)F}{RT}\eta - \ln\left(\frac{1-\theta_0}{1-\theta}\right)\right\}\right]. \tag{4}$$

When the total polarization loss is small, the exponential functions can be approximated to be linear, that is

$$\exp\left\{\frac{2\beta F}{RT}\eta + \ln\left(\frac{\theta}{\theta_0}\right)\right\} \approx 1 + \frac{2\beta F}{RT}\eta + \ln\left(\frac{\theta}{\theta_0}\right). \tag{5}$$

A similar approximation being applied to the second term, we obtain

$$i = i_0\left\{\frac{2F}{RT}\eta + \ln\left(\frac{\theta}{\theta_0}\right)\left(\frac{1-\theta_0}{1-\theta}\right)\right\}. \tag{6}$$

Rearranging yields

$$\eta = \frac{RT}{2Fi_0}i - \frac{RT}{2F}\ln\left(\frac{\theta}{\theta_0}\right)\left(\frac{1-\theta_0}{1-\theta}\right), \tag{7}$$

or

$$\eta = \eta_{ct} + \eta_c, \tag{8}$$

where

$$\eta_{ct} = \frac{RT}{2Fi_0}i, \qquad \eta_c = -\frac{RT}{2F}\ln\left(\frac{\theta}{\theta_0}\right)\left(\frac{1-\theta_0}{1-\theta}\right).$$

η_{ct} and η_c are the charge transfer polarization and concentration polarization, respectively. Equation (8) indicates that the total polarization loss is the sum of the two polarization losses.

When the steady current is interrupted, the double layer starts to be discharged, so that the charge transfer polarization decreases with time, according to the decay equation

$$\frac{d\eta_{ct}}{dt} = -\frac{i}{C_{dl}}. \tag{9}$$

Integration of Eq. 9 by considering $\eta_{ct} = RTi/2Fi_0$ and combination with Eq. 8 give

$$\eta = (\eta_0 - \eta_c)\exp\left(-\frac{t}{R_pC_{dl}}\right) + \eta_c, \tag{10}$$

where $R_p = RT/2Fi_0$ and η_0 is η at $t=0$.

As seen from Eq. 10, when the concentration polarization η_c is negligibly small, the decay curve will be linear on the $\log\eta$ vs. t plots. This is the case for the discharge of a simple R–C parallel circuit. To obtain a complete decay equation, it is necessary to express η_c as a function of the decay time.

There are two possible rate controlling steps in the reaction mechanism described above; surface diffusion of O_a and dissociation of O_2. Which of the two is a dominant factor can be determined by the steady state measurements. When the electrode reaction in question is controlled by the diffusion of O_a, the steady current density is given by Fick's first law, so that

$$\frac{i_s}{2F} = D\frac{\theta_0 - \theta_s}{l}, \tag{11}$$

where the subscript s refers to the steady state. The limiting current density i_L is obtained as the current density for $\theta_s = 0$

$$\frac{i_L}{2F} = \frac{D\theta_0}{l}, \tag{12}$$

Dividing Eq. 11 by Eq. 12 yields

$$\frac{i_s}{i_L} = 1 - \frac{\theta_s}{\theta_0}, \tag{13}$$

For a relatively low oxygen pressure and high operating temperature, one can assume $\theta \ll 1$, so that $(1-\theta)/(1-\theta_0) \approx 1$.[4,7,8] Substitution of Eq. 13 into Eq. 3 by assuming this approximation gives

$$i_s = i_0\left\{\left(1 - \frac{i_s}{i_L}\right)\exp\left(\frac{2\beta F}{RT}\eta\right) - \exp\left(-\frac{2(1-\beta)F}{RT}\eta\right)\right\}. \tag{14}$$

On the other hand, if the electrode process is limited by the dissociation of O_2 molecules, the steady current corresponds to the dissociation rate of O_2 molecules subtracted by the recombination rate of O_a atoms, that is,

$$\frac{i_s}{4F}=k_1(1-\theta_0)\left\{\frac{1-\theta_s}{1-\theta_0}-\left(\frac{\theta_s}{\theta_0}\right)^2\right\}, \quad (15)$$

where k_1 is the rate constant of dissociation. For the case $\theta \ll 1$, Eq. 15 becomes

$$\frac{i_s}{4F}=k_1(1-\theta_0)\left\{1-\left(\frac{\theta_s}{\theta_0}\right)^2\right\}, \quad (16)$$

The limiting current density is obtained for $\theta_s=0$,i.e., $i_L=4Fk_1(1-\theta_0)$, so that

$$\frac{i_s}{i_L}=1-\left(\frac{\theta_s}{\theta_0}\right)^2. \quad (17)$$

Inserting the above equation into Eq. 3 by assuming $(1-\theta)/(1-\theta_0)=1$ gives

$$i_s=i_0\left\{\sqrt{1-\frac{i_s}{i_L}}\exp\left(\frac{2\beta F}{RT}\eta\right)-\exp\left(-\frac{2(1-\beta)F}{RT}\eta\right)\right\}. \quad (18)$$

The steady state polarization curves for diffusion limiting and dissociation limiting are thus expressed in Eq. 14 and 18, respectively. Figure 2 shows a steady state polarization data selected from Fig. 5. Solid lines 1 and 2 are the best fit curves calculated from Eqs. 14 and 18, respectively, using $\beta=0.5$. The values of i_L and i_0 used are indicated in the caption. It is seen that the equation for the dissociation limiting gives too small i_L value while that for diffusion limiting agrees better with the experimental plots. This means that the concentration polarization is mainly due to the diffusion of O_a atoms.

Inserting Eq. 13 into Eq. 7, and approximating $\ln(1-i_s/i_L)=i_s/i_L$ and $(1-\theta)/(1-\theta_0)=1$ yields

$$\eta=\frac{RTi_s}{2F}\left(\frac{1}{i_0}+\frac{1}{i_L}\right) \quad (19)$$

This equation gives the approximate proportion of each loss. As seen in the caption of Fig. 2, the best fit value of i_0 is much greater than that of i_L, that is, $1/i_0 \ll 1/i_L$ in the above equation, so that the charge transfer polarization is negligibly small in comparison with the concentration polarization. Thus, it follows that the polarization loss of the electrodes used consists of the concentration polarization which is due to the diffusion of O_a atoms. A decay equation will be derived on the basis of the diffusion mechanism, as described below.

Atomic oxygen O_a formed by the dissociative adsorption diffuses over a diffusion length l to three phase boundaries. (In this analysis, the important factor is the diffusion species, and not the diffusion path, so that the question on the diffusion path of O_a atom is not considered in detail. The platinum surface and electrode–electrolyte interface have been proposed as probable diffusion paths.[7-11]) For this case, the concentration–distance profile is such as shown in Fig. 3, where C_0

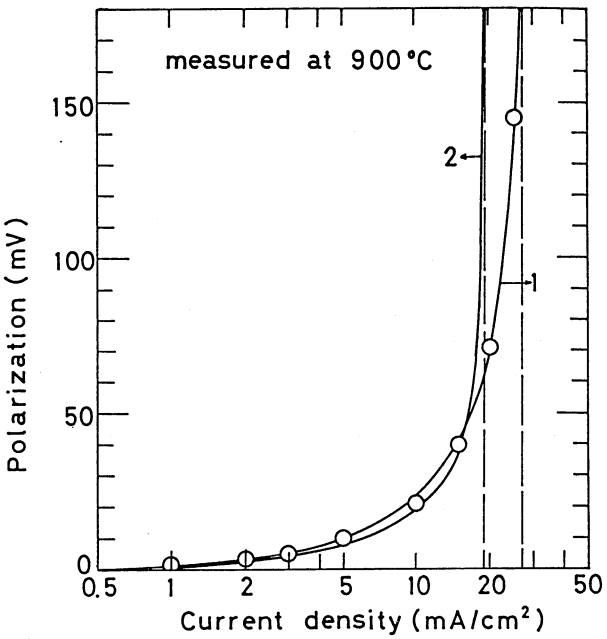

Fig. 2. Comparison of experimental polarization data (open circles) with theoretical polarization curves calculated from the diffusion mechanism (Curve 1, i_L=27 mA cm^{-2} and i_0=1 A cm^{-2} were assumed) and dissociation mechanism (Curve 2, i_L=19 mA cm^{-2} and i_0=1 A cm^{-2} were assumed). Experimental data were selected from Fig. 5 (P_{O_2}=0.01 atm).

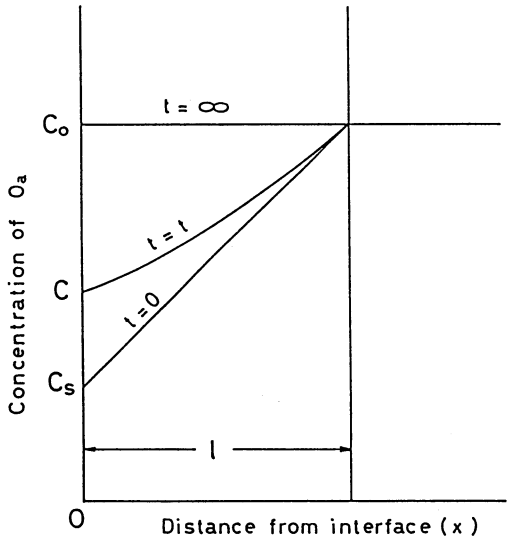

Fig. 3. Schematic profile of the concentration gradient in the diffusion path.

and C_S are concentrations of O_a for equilibrium and steady-state conditions, respectively. When the steady current is interrupted, C_S begins to increase toward C_0. For this transient process, C must satisfy Fick's second law of diffusion

$$\frac{\partial C}{\partial t}=D\frac{\partial^2 C}{\partial x^2}, \quad (20)$$

associated with the following boundary conditions

$$C=\frac{C_0-C_S}{l}x+C_S \quad \text{at } t=0, \tag{21}$$

$$D\frac{\partial C}{\partial x}=A\delta\frac{\partial C}{\partial t} \quad \text{at } x=0, \tag{22}$$

$$C=C_0 \quad \text{at } x=l. \tag{23}$$

Equation (21) is a concentration-distance relationship in the steady state. Equation (22) results from a mass balance at the electrode-electrolyte interface. When the steady current is interrupted, the reduction (consumption) of O_a ceases, so that O_a begins to accumulate in the electrode-electrolyte interface. The amount of O_a transported to the interface by diffusion for dt sec is $D(\partial C/\partial x)$dt. This amount must be balanced with the amount of O_a accumulated in the interface, i.e., $A\delta$dC, where A is the interfacial area per 1 cm^2 of nominal electrode area and δ is the thickness of monolayer of O_a. Equating these two terms leads to Eq. 22.

The dimensionless forms of the above respective questions are

$$\frac{\partial \Pi}{\partial \tau}=\frac{\partial^2 \Pi}{\partial \xi^2} \tag{24}$$

$$\Pi=\xi \quad \text{at } \tau=0, \tag{25}$$

$$\frac{\partial \Pi}{\partial \xi}=\alpha\frac{\partial \Pi}{\partial \tau} \quad \text{at } \xi=0, \tag{26}$$

$$\Pi=1 \quad \text{at } \xi=1, \tag{27}$$

where $\Pi=(C-C_S)/(C_0-C_S)$, $\tau=Dt/l^2$, $\xi=x/l$, and $\alpha=A\delta/l$. Laplace transformation of Eq. 24 using Eq. 25 gives

$$\frac{d^2F(S)}{d\xi^2}=sF(s)-\xi, \tag{28}$$

where $F(s)=\mathcal{L}\{\Pi(\tau)\}$. Only the solution of Eq. 28 at the interface $\xi=0$ directly controls the electrode potential, so that

$$F(s,\xi=0)=\frac{\tanh\sqrt{s}}{s\sqrt{s}\,(1+\alpha\sqrt{s}\,\tan\sqrt{s}\,)}. \tag{29}$$

Inverse transformation of Eq. 29 is not easy, so that Alfrey's approximation formula was used to obtain an approximate solution,[12] that is,

$$\Pi(\tau)=\left\{-s^2\frac{dF(s)}{ds}\right\}_{s=1/\tau}, \tag{30}$$

or in a higher degree of approximation

$$\Pi(\tau)=\left\{s^2\frac{d^2F(s)}{ds^2}\right\}_{s=2/\tau}, \tag{31}$$

Substitution of Eq. 29 into Eq. 30 and considering $\tau=Dt/l^2=t/t_0$ lead to the solution as follows

$$\Pi(\tau)_{\tau=t/t_0}=\pi(t)$$
$$=\frac{1}{2(1+\alpha\sqrt{t_0/t}\tanh\sqrt{t_0/t})^2}\left\{\left(\frac{3}{\sqrt{t_0/t}}+4\alpha\tanh\sqrt{t_0/t}\right.\right.$$
$$\left.+\alpha(t_0/t)^{3/2}\operatorname{sech}^2\sqrt{t_0/t}-\alpha\sqrt{t_0/t}\operatorname{sech}^2\sqrt{t_0/t}\right)\tanh\sqrt{t_0/t}$$
$$-\operatorname{sech}^2\sqrt{t_0/t}. \tag{32}$$

The actual calculation was performed using the more accurate solution obtained from Eq. 31 although its full expression is too complicated to write here. Assuming $\theta_s/\theta_0=C_s/C_0$ and $\theta/\theta_0=C/C_0$ and substituting these into Eq. 14 and the definition $\Pi=(C-C_s)/(C_0-C_s)$, we obtain

$$\frac{C}{C_0}=1-\frac{i_s}{i_L}\{1-\Pi(t)\}. \tag{33}$$

This equation expresses the time variation of concentration of O_a at the three phase boundary, so that the decay equation required is obtained by inserting Eq. 33 into the Nernst equation

$$\eta_c=-\frac{RT}{2F}\ln\frac{C}{C_0}=-\frac{RT}{2F}\ln\left\{1-\frac{i_s}{i_L}(1-\Pi(t))\right\}. \tag{34}$$

Equation (34) is the final form of decay equation, which involves three parameters, i_L, i_0 ($=l^2/D$), and α ($=A\delta/l$). The parameter i_L is the limiting current density whose meaning is obvious. t_0 is the time constant determining the decay rate, or slope of the decay curve. α involves the interfacial area and hence it can be used

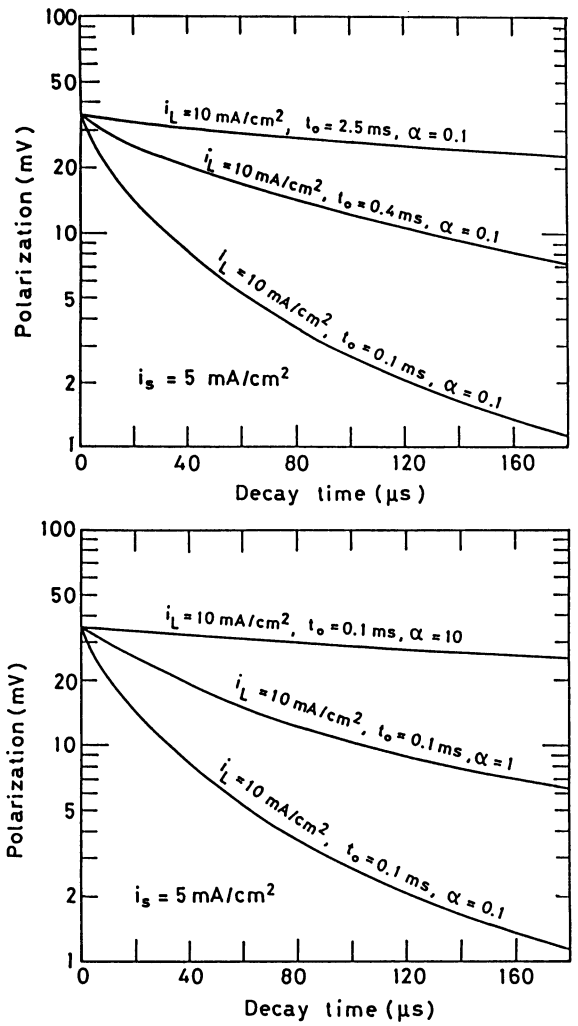

Fig. 4. Theoretical decay curves calculated for variations of t_0 (top) and α (bottom). Temperature: 900 °C.

as a measure of the effective reaction area of the electrode. As the reaction area for charge transfer, i.e., electrode-electrolyte interface, becomes larger, it will take a longer time for O_a to accumulate in the interface. This means that the decay rate will be slower for the electrode having a larger reaction area. To test these predictions, decay curves were calculated from Eq. 34 using several t_0 and α values chosen arbitrarily. Results of the calculation are shown in Fig. 4. It is seen that the decay rate becomes faster as t_0 and α decrease as predicted above.

Experimental data were obtained in a series of discrete values of polarizations vs. time. The sum of the difference between the theoretical and experimental polarizations obtained for every t value given in the experimental data, that is, $\Sigma|\eta_{theor}-\eta_{exp}|$, was used as a measure of the goodness of fit of the theoretical curves for the parameter values used. Calculation of the error functions was repeated for every combination of the parameter values given until the best-fit parameter values that minimize these measures were found. Final determination of the best-fit values was made by the Powell method of conjugated directions[13] using the parameter values obtained above as initial values. This method could enhance significantly the accuracy of parameter values, although the goodness of fit also depends on the scattering of experimental data used.

Application to Pt/ZrO_2 Electrodes

Platinum electrodes sintered on zirconia electrolytes are suitable to test the theory described above, because they give reliable and reproducible polarization data. Figure 5 shows the steady state polarization curves of Pt/ZrO_2 electrodes in various oxygen pressures. Solid lines are calculated from Eq. 14 by adjusting the i_L value. A good agreement between the calculated and experimental values can be seen, indicating that the diffusional polarization loss is a major polarization component, as described previously.

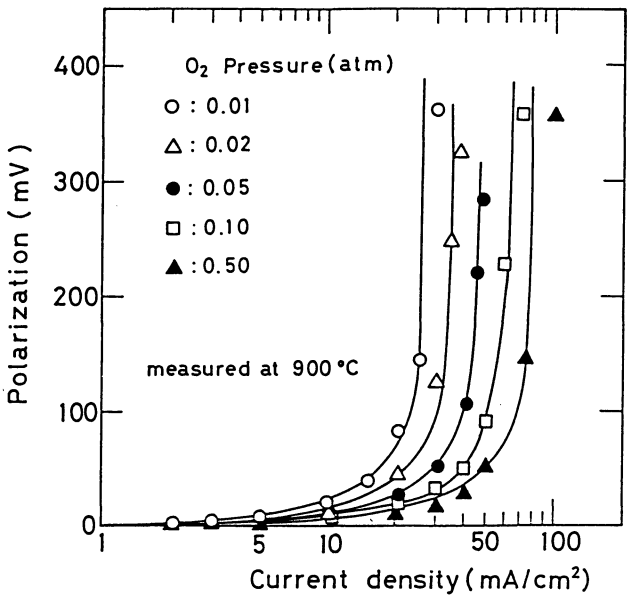

Fig. 5. Steady state polarization curves of Pt/ZrO_2 oxygen cathodes for various oxygen pressures. Solid lines indicate the best fit curves calculated from Eq. 12.

Figure 6 gives the corresponding decay curves of the same electrodes. Solid lines are the best fit curves obtained from Eq. 34. The parameter values used for the best fit are summarized in Table 1. It is seen that α is almost independent of P_{O_2}, suggesting that the effective reaction area is invariant with P_{O_2}. The expected relationship between i_L and P_{O_2} can be derived from Eq. 12. Combination of Eq. 12 with mass action law, i.e., θ_0^2/P_{O_2}=constant, leads to $i_L \propto D\sqrt{P_{O_2}}/l$, so that one can expect that the log-log plots of i_L vs. P_{O_2} fall on a straight line having the 1/2 slope. Such plots are shown in Fig. 7, where the expected trend can be seen. The calculated i_L values agree well with the experimental ones. These facts are in favor of the diffusion mechanism assumed at the beginning of the analysis, and also agrees with the interpretation widely accepted.[14]

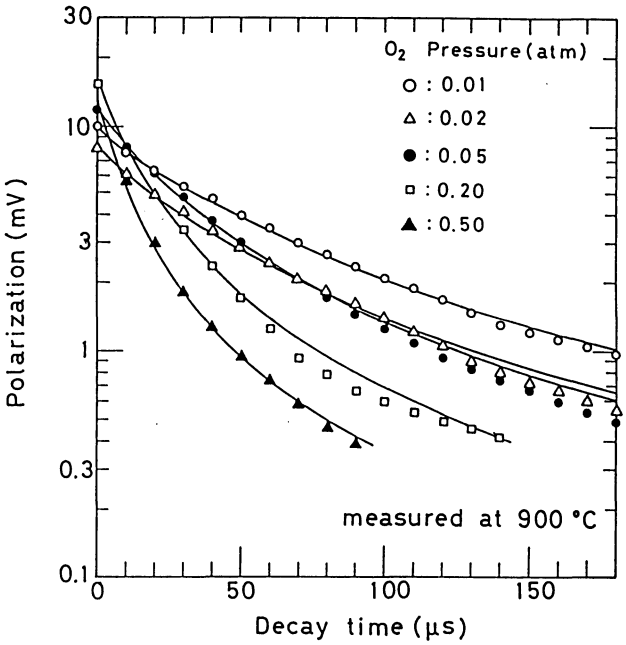

Fig. 6. Decay curves of Pt/ZrO_2 oxygen cathodes for various oxygen pressures. Solid lines indicate the best fit curves calculated from Eq. 32.

Table 1. Dependence of Parameter Values on the Oxygen Pressure

P_{O_2}/atm	i_L/mA cm^{-2}	t_o/ms	α	R_p/Ω cm^2
0.01	27.5	0.20	0.08	1.98
0.02	33	0.15	0.13	1.62
0.05	47.6	0.104	0.15	1.15
0.10	59.5	0.087	0.11	0.973
0.20	75	0.059	0.12	0.759
0.50	85	0.039	0.12	0.591

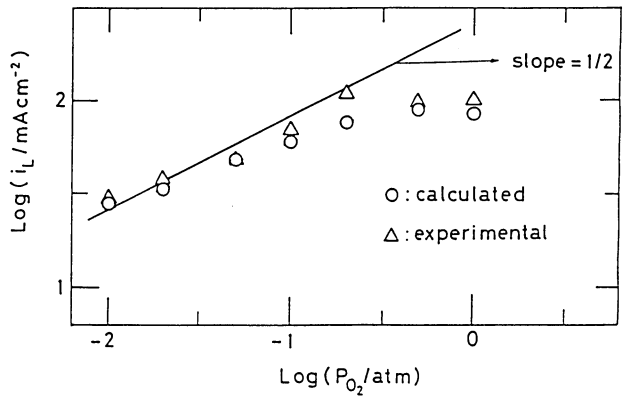

Fig. 7. Log–log plots of i_L vs. P_{O_2}. Data obtained from Table 1.

Table 2. Effects of Sintering Temperature on the Parameter Values (measured at 900 °C in P_{O_2}=0.2 atm)

Sintering tempeature (°C)	R_p/Ω cm^2	i_L/mA cm^{-2}	t_0/ms	α
900	0.47	108	0.031	0.29
1000	0.38	130	0.031	0.60
1200	0.31	166	0.031	0.57
1300	0.26	205	0.030	1.10

The Pt particles were found to grow in size as the sintering temperature rises.[5] It is expected that this size effect influences the decay curve, and hence the parameter values. To examine this effect, platinum paste was sintered on the zirconia disks at various temperatures for 1 h. The results obtained are given in Table 2. It is seen that the polarization loss (R_p) essentially decreases with increasing sintering temperature. In the relation between R_p and α, one can see that the decrease in the loss is associated with an increase in α. Remembering that α is defined as $A\delta/l$, α can be a measure of the effective reaction area. The parallel relationship between α and sintering temperature therefore means that the electrode–electrolyte interface increases with the progress of sintering. This may be due to an improved contact of Pt particles to the electrolyte disk.

It is well known that the performance of electrode is enhanced by applying an excess load current on the electrode.[15–17] This current passage effect has been reasoned by several authors.[16,18] The explanation most widely believed is that the effective reaction area increases because a part of the electrolyte near the interface becomes an electronic-ion mixed conductor.[18] To test the validity of this explanation, the analytical method was applied to a Pt/ZrO_2 electrode which was subjected to a preliminary treatment by an excess current. The current passage effect for the Pt/ZrO_2 electrode is shown in Fig. 8, where the polarization resistance, which was experimentally obtained by dividing the polarization by the current density, is used as a measure

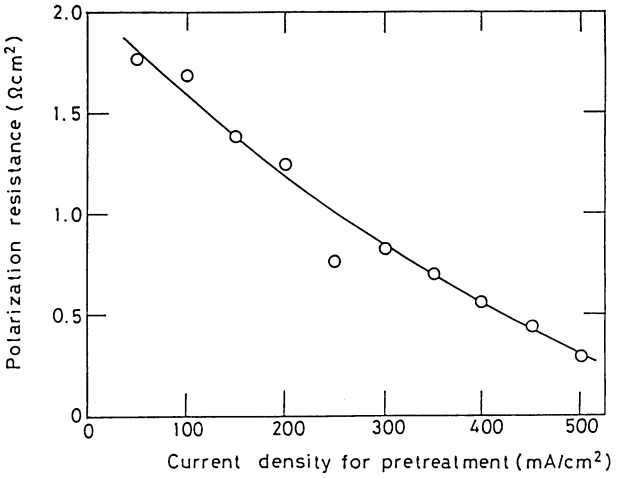

Fig. 8. Current passage effect for Pt/ZrO_2 oxygen cathodes. Polarization resistance is plotted as a measure of the performance against the current density passed before the measurement in direction of cathodic polarization. Polarization measured at 900 °C in air.

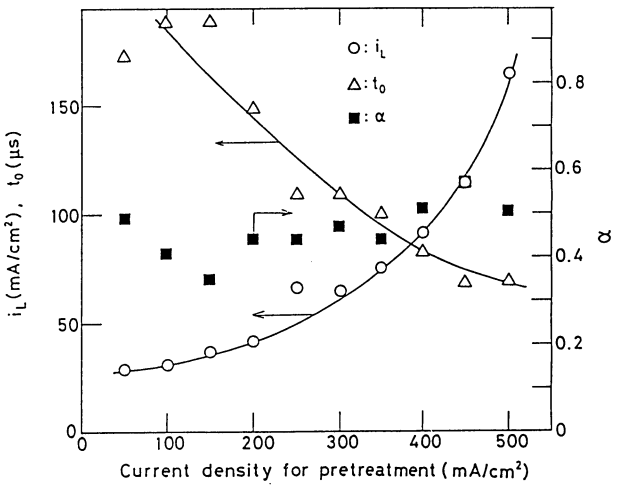

Fig. 9. Current passage effect on the parameter values. The values of i_L, t_0, and α for the same electrodes as in Fig. 8 are plotted against the current density for pretreatment.

of the performance. Obviously, the performance is increased with increasing current. The parameter values obtained from the decay curves are given as a function of the current in Fig. 9. The performance improvement reflects on an increase in i_L. It should be noted that α is almost constant while t_0 decreases with increasing treating current. This suggests, in contrary to the usual explanation, that the current passage effect is not due to a change of reaction area, but to an increase in the diffusivity.

Conclusion

The steady state polarization curves of Pt/ZrO_2 oxy-

gen electrodes were measured as a function of P_{O_2}, and then i_L and i_0 were determined by curve fitting to the Butler-Volmer equation. The estimated values suggest that the polarization loss is mainly controlled by the diffusion of atomic oxygen. Based on the diffusion mechanism, a decay equation was derived as an approximate solution of Fick's second law of diffusion. The theoretical decay curves calculated from the equation fit the experimental decay curves by adjusting parameters involved in the equation. The i_L values obtained from the equation agree well with the experimental ones, and the log-log plots of i_L vs. P_{O_2} fall on a line having the slope of 1/2. These findings agree with the diffusion mechanism assumed. The decay equation involves a measure of the effective reaction area. This measure was tested by applying this equation to a series of Pt electrodes prepared in various sintering temperatures. Results of the analysis indicate that the reaction area increases with sintering temperature. This is to be expected from the observation that the Pt particles grow in size as the sintering temperature rises. The electrode treated by an excess current passage enhanced the performance. This effect was found to be ascribed to the diffusivity of O_a rather than the reaction area.

Nomenclature

A interfacial area (cm^2/cm^2 of electrode)
C concentration of O_a ($mol\,cm^{-3}$)
C_0 C at equilibrium state ($mol\,cm^{-3}$)
C_s C at steady state ($mol\,cm^{-3}$)
C_{dl} double layer capacity ($\mu F\,cm^{-2}$)
D diffusion constant of O_a ($cm^2\,s^{-1}$)
F Faraday constant (96487C/equiv)
$F(s)$ Laplace transform of $\Pi(\tau)$, or $\mathscr{L}\{\Pi(\tau)\}$
i current density ($mA\,cm^{-2}$)
i_0 exchange current density ($mA\,cm^{-2}$)
i_s steady state current density ($mA\,cm^{-2}$)
i_L limiting current density ($mA\,cm^{-2}$)
k_1 rate constant of dissociation
l diffusion length of O_a (cm)
O_a adsorbed oxygen atom
P_{O_2} oxygen partial pressure (atm)
R gas constant ($8.314J\,K^{-1}\,mol^{-1}$)
R_p polarization resistance ($\Omega\,cm^2$)
T temperature (K)
t decay time (s)
t_0 time constant, or l^2/D (s)
x diffusion distance (cm)
α $A\delta/l$
β transfer coefficient
δ thickness of monolayer of O_a (cm)
η total polarization (mV)
η_0 total polarization at $t=0$
η_c concentration polarization (mV)
θ coverage of of O_a
θ_0 θ at equilibrium state
θ_s θ in the steady state
ξ x/l
$\Pi(\tau)$ $(C-C_s)/(C_0-C_s)$
τ Dt/l^2

References

1) D. T. Hooie, in "Proceedings of the Conference on the High Temperature Solid Oxide Electrolytes," Brookhaven National Laboratory, Upton, New York (1983), Vol. 1, p. 17.
2) K. V. Kordesch and A. Marko, *J. Electrochem. Soc.*, **107**, 480 (1960).
3) P. H. Bottelberghs, "Solid Electrolytes," ed by P. Hagenmuller and W. van Gool, Academic Press, New York (1978), p. 145.
4) D. Y. Wang and A. S. Nowick, *J. Electrochem. Soc.*, **126**, 1166 (1979).
5) T. Kenjo, Y. Horiuchi, and S. Osawa, *J. Electrochem. Soc.*, **137**, 2423 (1990).
6) K. V. Vetter, "Electrochemical Kinetics," Academic Press, New York (1967), p. 342.
7) B. C. Ngugen, L. M. Rincon-Rubio, and D. M. Mason, *J. Electrochem. Soc.*, **133**, 1860 (1986).
8) J. Mizusaki, K. Amano, S. Yamauch, and K. Fueki, *Solid State Ionics*, **22**, 313 (1987).
9) D. Braunshtein, D. S. Tannhauser, and I. Riess, *J. Electrochem. Soc.*, **128**, 82 (1981).
10) G. B. Barbi and F. Beonio-Brocchieri, *Ber. Bunsen-Ges. Phys. Chem.*, **92**, 36 (1988).
11) W. Gopel and H. Wiemhofer, *Ber. Bunsen-Ges. Phys. Chem.*, **94**, 981 (1990).
12) A. Popoulis, *Q. Appl. Math.*, **14**, 405 (1957).
13) M. J. D. Powell, *Comput. J.*, **7**, 155 (1964).
14) B. C. H. Steele, in "Electrode Process in Solid State Ionics," Proceedings of the NATO advanced Study Institute, ed by M. Kleitz and J. Dupuy, D. Reidel Publishing Company, Dordrecht, Holland (1976), p. 367.
15) T. Takahashi, H. Iwahara, and I. Ito, *Denki Kagaku*, **38**, 288 (1970).
16) T. Takahashi, H. Iwahara, and I. Ito, *Denki Kagaku*, **38**, 509 (1970).
17) M. V. Perfil'v, S. F. Pal'guev, "Electrochem. of Molten and Solid Electrolytes," Trans. No. 6 of the Inst. Electrochem. Urals Akad. Sci., (1966), Vol. 3, p. 105.
18) K. P. Jagannathan, S. K. Tiku, H. S. Ray, A. Ghosh, and E. C. Subbarao, "Solid Electrolytes and Their Application," ed by E. C. Subbarao, Plenum Press, New York and London (1980), p. 201.